Comparison of *p*-*p*, *p*-Pb, and Pb-Pb collisions in the thermal model: Multiplicity dependence of thermal parameters

Natasha Sharma,[1] Jean Cleymans,[2] Boris Hippolyte,[3] and Masimba Paradza[2]
[1]*Department of Physics, Panjab University, Chandigarh 160014, India*
[2]*UCT-CERN Research Centre and Department of Physics, University of Cape Town, Rondebosch 7701, South Africa*
[3]*Institut Pluridisciplinaire Hubert Curien and Université de Strasbourg Institute for Advanced Study, CNRS-IN2P3, Strasbourg, France*

(Received 5 November 2018; published 22 April 2019)

An analysis is made of the particle composition (hadrochemistry) of the final state in proton-proton (*p*-*p*), proton-lead (*p*-Pb) and lead-lead (Pb-Pb) collisions as a function of the charged particle multiplicity ($dN_{\rm ch}/d\eta$). The thermal model is used to determine the chemical freeze-out temperature as well as the radius and strangeness saturation factor γ_s. Three different ensembles are used in the analysis; namely, the grand canonical ensemble, the canonical ensemble with exact strangeness conservation, and the canonical ensemble with exact baryon number, strangeness, and electric charge conservation. It is shown that for high multiplicities (at least 20 charged hadrons in the midrapidity interval considered) the three ensembles lead to the same results.

DOI: 10.1103/PhysRevC.99.044914

I. INTRODUCTION

In high-energy collisions, applications of the thermal-statistical model in the form of the hadron resonance gas model have been successful (see, e.g., Refs. [1,2] for two recent publications) in describing the composition of the final state, e.g., the yields of pions, kaons, protons, and other hadrons. In these descriptions use is made of the grand canonical ensemble and the canonical ensemble with exact strangeness conservation. In this paper we consider in addition the use of the canonical ensemble with exact baryon, strangeness and charge conservation. We also make a systematic analysis of the dependence on the charged particle multiplicity $dN_{\rm ch}/d\eta$.

The identifying feature of the thermal model is that all hadronic resonances listed in the summary tables in Ref. [3] are assumed to be in thermal and chemical equilibrium. This assumption drastically reduces the number of free parameters because this stage is determined by just a few thermodynamic variables; namely, the chemical freeze-out temperature $T_{\rm ch}$ and the various chemical potentials μ determined by the conserved quantum numbers and by the volume V of the system. It has been shown that this description is also the correct one [4–6] for a scaling expansion as first discussed by Bjorken [7].

After integration over p_T these authors have shown that

$$\frac{dN_i/dy}{dN_j/dy} = \frac{N_i^0}{N_j^0}, \tag{1}$$

where N_i^0 (N_j^0) is the particle yield of hadron i (j) as calculated in a fireball at rest, while dN_i/dy is the yield of hadron i on the rapidity plateau. Hence, in the Bjorken model with longitudinal scaling and radial expansion, the effects of hydrodynamic flow cancel out in ratios.

The yields produced in heavy-ion collisions have been the subject of intense discussions over the past few years and several proposals have been made in view of the fact that the number of pions is underestimated while the number of protons is overestimated. Several proposals to improve on this have been made recently:

1. incomplete hadron spectrum [8];
2. chemical nonequilibrium at freeze-out [9–11];
3. modification of hadron abundances in the hadronic phase [12–14];
4. separate freeze-out for strange and nonstrange hadrons [15–18];
5. excluded volume interactions [19];
6. energy dependent Breit–Wigner widths [20];
7. the use the phase shift analysis to take into account repulsive and attractive interactions [21,22];
8. the use the K-matrix formalism to take interactions into account [23].

These proposals improve the agreement with the observed yields and, furthermore, some of them change the chemical freeze-out temperature $T_{\rm ch}$ in only a minimal way, such as those presented recently in Refs. [20,22]. In the present analysis we therefore kept to the basic structure of the thermal model with a single freeze-out temperature and focus on

the resulting thermal parameters $T_{\rm ch}$, γ_s and the radius. All our calculations were done by using the latest version of THERMUS [24].[1]

Our results show some interesting new features:

1. The grand canonical ensemble, the ensemble with strict strangeness conservation, and the one with strict baryon number, strangeness, and charge conservation agree very well for the particle composition in Pb-Pb collisions; they also agree well for p-Pb collisions but marked differences for p-p collisions are present. These differences disappear as the multiplicity of charged particles increases in the final state. Thus, p-p collisions with high multiplicities agree with what is seen in large systems such as p-Pb and Pb-Pb collisions. Quantitatively, this agreement starts when there are at least 20 charged hadrons in the midrapidity interval being considered. It also throws doubt on the applicability of the thermal model as applied to p-p collisions with low multiplicity.
2. The convergence of the results in the three ensembles lends support to the idea that one reaches a thermodynamic limit where the results are independent of the ensemble being used.

II. ENSEMBLES CONSIDERED IN THE THERMAL MODEL

We compare in great detail three different ensembles based on the thermal model. In the following we consistently use the Boltzmann approximation; the actual numerical calculations use quantum statistics as far as possible.

1. In the grand canonical ensemble (GCE), the conservation of quantum numbers is implemented by using chemical potentials. The quantum numbers are conserved on average. The partition function depends on thermodynamic quantities and the Hamiltonian describing the system of N hadrons:

$$Z_{\rm GCE} = {\rm Tr}[e^{-(H-\mu N)/T}], \tag{2}$$

which, in the framework of the thermal model considered here, leads to

$$\ln Z_{\rm GCE}(T,\mu,V) = \sum_i g_i V \int \frac{d^3p}{(2\pi)^3} \exp\left(-\frac{E_i-\mu_i}{T}\right) \tag{3}$$

in the Boltzmann approximation, where g_i is the degeneracy factor of hadron i, V is the volume of the system, and μ_i is the chemical potential associated with the hadron. The yield is given by

$$N_i^{\rm GCE} = g_i V \int \frac{d^3p}{(2\pi)^3} \exp\left(-\frac{E_i}{T}\right), \tag{4}$$

where we have put the chemical potentials equal to zero, as is relevant for the beam energies at the Large Hadron Collider considered here. The decays of resonances have to be added to the final yield:

$$N_i^{\rm GCE}({\rm total}) = N_i^{\rm GCE} + \sum_j Br(j\to i) N_j^{\rm GCE}. \tag{5}$$

2. Canonical ensemble with exact implementation of strangeness conservation, we will refer to this as the strangeness canonical ensemble (SCE). There are chemical potentials for baryon number B and charge Q but not for strangeness:

$$Z_{\rm SCE} = {\rm Tr}\left[e^{-(H-\mu N)/T}\delta_{(S,\sum_i S_i)}\right]. \tag{6}$$

The δ function imposes exact strangeness conservation, requiring overall strangeness to be fixed to the value S. In this paper we will only consider the case where overall strangeness is zero, $S=0$. This change leads to [25]

$$Z_{\rm SCE} = \frac{1}{(2\pi)}\int_0^{2\pi} d\phi e^{-iS\phi} Z_{\rm GCE}(T,\mu_B,\lambda_S), \tag{7}$$

where the fugacity factor is replaced by

$$\lambda_S = e^{i\phi}, \tag{8}$$

$$N_i^{\rm SCE} = V\frac{Z_i^1}{Z_{S=0}^C}\sum_{k,p=-\infty}^{\infty} a_3^p a_2^k a_1^{-2k-3p-s} \times I_k(x_2) I_p(x_3) I_{-2k-3p-s}(x_1), \tag{9}$$

where $Z_{S=0}^C$ is the canonical partition function,

$$Z_{S=0}^C = e^{S_0}\sum_{k,p=-\infty}^{\infty} a_3^p a_2^k a_1^{-2k-3p} I_k(x_2) I_p(x_3) I_{-2k-3p}(x_1),$$

where Z_i^1 is the one-particle partition function calculated for $\mu_S=0$ in the Boltzmann approximation. The arguments of the Bessel functions $I_s(x)$ and the parameters a_i are introduced as

$$a_s = \sqrt{S_s/S_{-s}}, \quad x_s = 2V\sqrt{S_s S_{-s}}, \tag{10}$$

where S_s is the sum of all $Z_k^1(\mu_S=0)$ for particle species k carrying strangeness s. As done previously, the decays of resonances have to be added to the final yield:

$$N_i^{\rm SCE}({\rm total}) = N_i^{\rm SCE} + \sum_j Br(j\to i) N_j^{\rm SCE}. \tag{11}$$

3. Canonical ensemble with exact implementation of B, S, and Q conservation; we refer to this as the full canonical ensemble (FCE). In this ensemble there are no chemical potentials. The partition function is given by

$$Z_{\rm FCE} = {\rm Tr}\left[e^{-H/T}\delta_{(B,\sum_i B_i)}\delta_{(Q,\sum_i Q_i)}\delta_{(S,\sum_i S_i)}\right], \tag{12}$$

$$Z_{\rm FCE} = \frac{1}{(2\pi)^3}\int_0^{2\pi} d\alpha e^{-iB\alpha}\int_0^{2\pi} d\psi e^{-iQ\psi} \times \int_0^{2\pi} d\phi e^{-iS\phi} Z_{\rm GCE}(T,\lambda_B,\lambda_Q,\lambda_S), \tag{13}$$

[1]B. Hippolyte and Y. Schutz, https://github.com/thermus-project/thermus.

TABLE I. Comparison between measured and fitted values for *p-p* collisions at 7 TeV for V0M multiplicity class II [27].

Particle species	dN/dy (data)	dN/dy (model)		
		Canonical S	Canonical B, S, Q	Grand canonical
$\pi^{\pm}$	7.88 ± 0.38	6.78	6.76	6.96
K^0_S	1.04 ± 0.05	1.16	1.16	1.15
p, $(\bar{p})$	0.44 ± 0.03	0.50	0.50	0.50
Λ	0.302 ± 0.020	0.259	0.262	0.246
$\Xi^-(\bar{\Xi}^+)$	0.0358 ± 0.0023	0.035	0.035	0.036

where the fugacity factors have been replaced by

$$\lambda_B = e^{i\alpha}, \quad \lambda_Q = e^{i\psi}, \quad \lambda_S = e^{i\phi}. \tag{14}$$

As before, the decays of resonances have to be added to the final yield

$$N_i^{\mathrm{FCE}}(\mathrm{total}) = N_i^{\mathrm{FCE}} + \sum_j Br(j \to i) N_j^{\mathrm{FCE}}. \tag{15}$$

In this case the analytic expression becomes very lengthy and we refrain from writing it down here; it is implemented in the THERMUS program [24].

In all three case we have also taken into account the strangeness saturation factor γ_s [26] which enters as a multiplicative factor, raised to the power of the strangeness content, in the particle yields. Keeping this factor fixed at unity does not change the fixed message, only the resulting value of χ^2 is increased, indicating a worsening of the fits.

These three ensembles are applied to *p-p* collisions at 7 TeV in the central region of rapidity [27], to *p*-Pb collisions at 5.02 TeV [28,29], and to Pb-Pb collisions at 2.76 TeV [30–32] with particular focus on the dependence on the charged particle multiplicity. It is well known that in this kinematic region, one has particle-antiparticle symmetry and therefore there is no net baryon density and also no net strangeness. The different ensembles nevertheless give different results because of the way they are implemented. A clear size dependence is present in the results of the ensembles. In the thermodynamic limit they should become equivalent. Clearly there are other ensembles that could be investigated and also other sources of finite-volume corrections. We hope to address these in a future presentation.

A similar analysis was done in Refs. [33–35] for *p-p* collisions at 200 GeV but without the dependence on charged multiplicity.

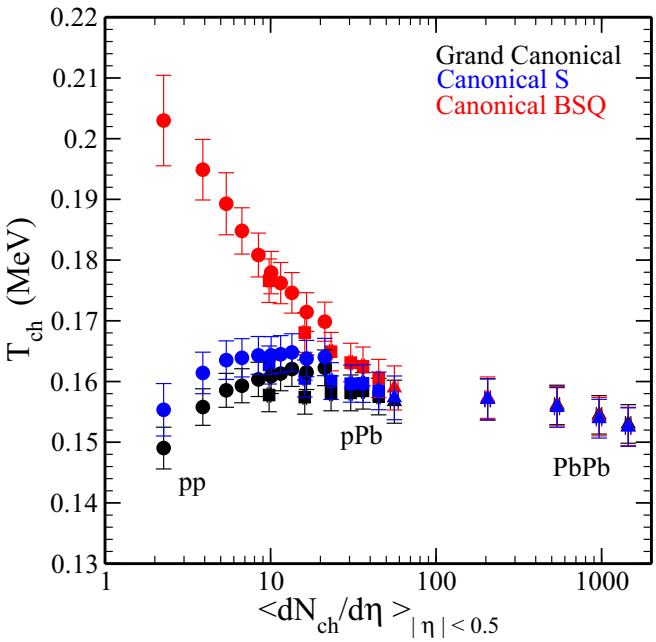

FIG. 1. The chemical freeze-out temperature T_{ch} obtained for three different ensembles. The black points are obtained by using the grand canonical ensemble, the blue points use exact strangeness conservation, while the red points have built-in exact baryon number, strangeness, and charge conservation. Circles are for *p-p* collisions at 7 TeV [27], squares are for *p*-Pb collisions at 5.02 TeV [28,29], while triangles are for Pb-Pb collisions at 2.76 TeV [30–32].

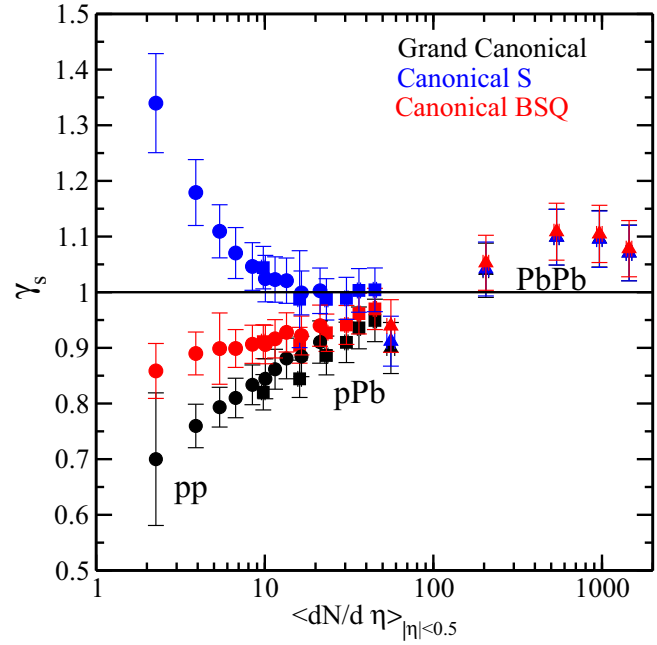

FIG. 2. The strangeness saturation factor γ_s obtained for three different ensembles. The black points were obtained by using the grand canonical ensemble, the blue points use exact strangeness conservation, while the red points have built-in exact baryon number, strangeness, and charge conservation. Circles are for *p-p* collisions at 7 TeV [27], squares are for *p*-Pb collisions at 5.02 TeV [28,29], while triangles are for Pb-Pb collisions at 2.76 TeV [30–32].

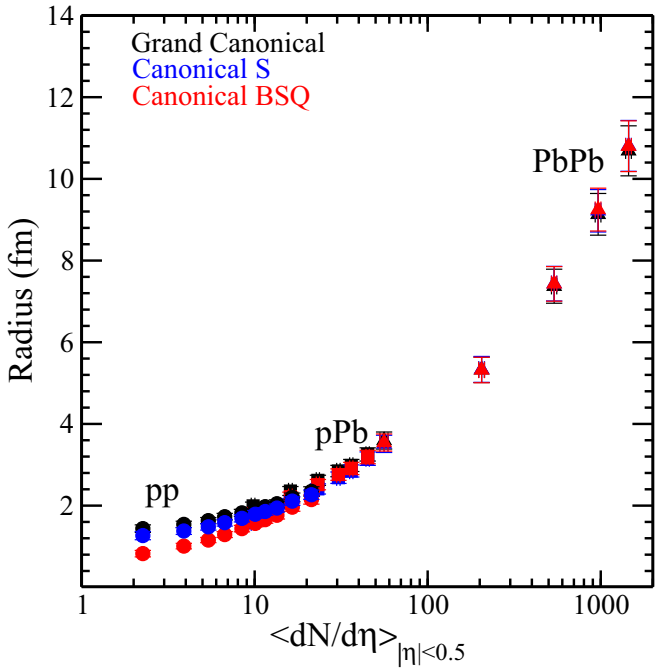

FIG. 3. The chemical freeze-out radius obtained for three different ensembles. The black points were obtained by using the grand canonical ensemble, the blue points use exact strangeness conservation, while the red points have built-in exact baryon number, strangeness, and charge conservation. Circles are for p-p collisions at 7 TeV [27], squares are for p-Pb collisions at 5.02 TeV [28,29], while triangles are for Pb-Pb collisions at 2.76 TeV [30–32].

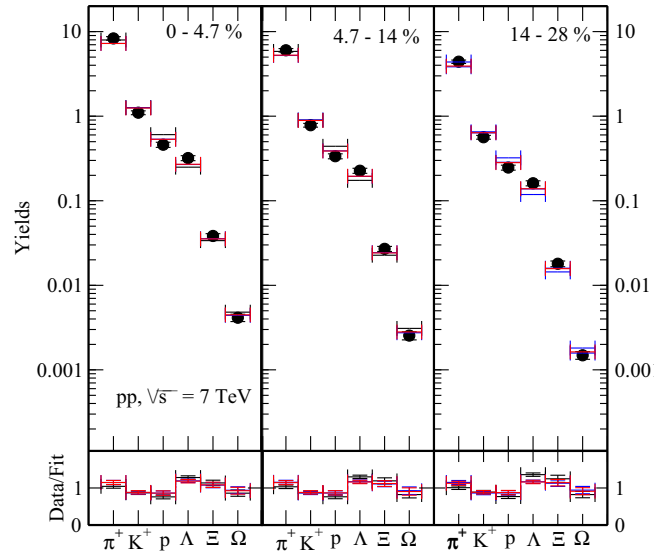

FIG. 4. Hadronic yields in p-p collisions at 7 TeV in centrality bins 1, 2, and 3 corresponding to 0%–4.7% (left panel) and 4.7%–14% (middle panel), and 14%–28% (right panel), respectively. The lower panel shows the ratio of experimental data divided by the fit results. The black points were obtained by using the grand canonical ensemble, the blue points use exact strangeness conservation, while the red ones have built-in exact baryon number, strangeness, and charge conservation. In some cases the bars overlap. The data are taken from Ref. [27].

For p-p collisions we have taken the five particle species listed in Table I where we also compare the measured values with the model calculations. For p-Pb and Pb-Pb collisions we included the Ω measurements in our analysis, so that six particle species were considered for p-Pb and Pb-Pb. We have checked explicitly that for the five bins in p-p collisions where Ω has also been measured, there is no difference in the outcome for the values of $T_{\rm ch}$, γ_s, and the radius.

As shown in Refs. [36,37], the ϕ meson is not described very well and has not been included.

III. COMPARISON OF DIFFERENT ENSEMBLES

In Fig. 1 we show the chemical freeze-out temperature as a function of the multiplicity of hadrons in the final state [27]. As explained in the previous section the freeze-out temperature has been calculated by using three different ensembles. The highest values are obtained by using the canonical ensemble with exact conservation of three quantum numbers, baryon number B, strangeness S, and charge Q, all of them being set to zero as is appropriate for the central rapidity region in p-p collisions at 7 TeV. In this ensemble the temperature drops strongly from the lowest to the highest multiplicity.

The lowest values for $T_{\rm ch}$ are obtained when using the grand canonical ensemble; in this case the conserved quantum numbers are again zero. The results are clearly different from those obtained in the previous ensemble, especially in the low-multiplicity intervals. They gradually approach each other and they become equal at the highest multiplicities.

For comparison with the previous two cases we also calculated $T_{\rm ch}$ by using the canonical ensemble with only strangeness S being exactly conserved by using the method presented in Ref. [25]. In this case the results are close to those obtained in the grand canonical ensemble, with the values of $T_{\rm ch}$ always slightly higher than in the grand canonical ensemble. Again for the highest multiplicity interval the results become equivalent.

The canonical BSQ ensemble leads to results which are incompatible with those obtained from lattice gauge theory [38], which indicate that hadrons cannot exist above the critical temperature which has been estimated to be about 156 ± 1.5 MeV. As can be seen in Fig. 1, even though all the ensembles produce different results, for high multiplicities the results converge to a common value close to 160 MeV.

In Fig. 2 we show results for the strangeness saturation factor γ_s [26]. In this case we obtain again quite substantial differences in each one of the three ensembles considered. The highest values being found in the canonical ensemble with exact strangeness conservation. Note that the values of γ_s become compatible with unity, i.e., with chemical equilibrium for all light flavors. Note that, for multiplicities, the value of γ_s is slightly above unity (by almost 10%) but is compatible with full chemical equilibrium within one standard deviation.

In Fig. 3 the radius at chemical freeze-out obtained in the three ensembles is presented. As in the previous figures, the results become independent of the ensemble chosen for

TABLE II. Values of χ^2/ndf for various fits discussed in the text. The degeneracy factors are different because Ω^- is not included in one set.

$\langle dN_{\rm ch}/d\eta\rangle\|_{\|\eta\|<0.5}$	Canonical S	Canonical B, S, Q	Grand canonical
		p-p collisions	
2.26	12.79/2	3.85/2	6.45/2
3.9	20.16/2	9.15/2	14.47/2
5.4	25.46/2	14.94/2	20.27/2
6.72	24.61/2	16.58/2	20.09/2
8.45	24.65/2	18.71/2	20.83/2
10.08	24.45/2	20.03/2	21.61/2
11.51	24.42/2	20.91/2	21.80/2
13.46	24.84/2	22.25/2	22.46/2
16.51	23.52/2	22.19/2	22.41/2
21.29	22.20/2	21.83/2	21.55/2
		p-Pb collisions	
9.8	22.37/3	17.86/3	18.72/3
16.1	20.07/3	19.36/3	21.10/3
23.2	19.23/3	19.71/3	20.60/3
30.5	18.23/3	19.23/3	19,76/3
36.2	18.17/3	19.39/3	19.42/3
45	18.43/3	19.81/3	20.26/3
		Pb-Pb collisions	
56	12.05/3	13.32/3	12.24/3
205	12.89/3	14.72/3	13.18/3
538	15.54/3	17.94/3	16.14/3
966	13.48/3	16.07/3	14.26/3
1448	11.08/3	13.07/3	11.45/3

the highest multiplicities while showing clear differences for low multiplicities.

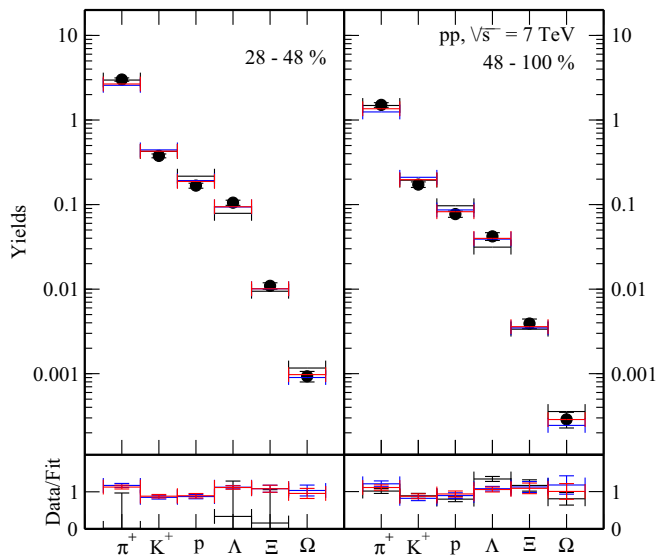

FIG. 5. Hadronic yields in *p-p* collisions at 7 TeV in centrality bins 4 and 5 corresponding to 28%–48% (left panel) and 48%–100% (right panel), respectively. The lower panel shows the ratio of experimental data divided by the fit results. The black bars were obtained by using the grand canonical ensemble, the blue ones use exact strangeness conservation, while the red ones have been obtained by using exact baryon number, strangeness, and charge conservation. The data are taken from Ref. [27].

Our results show that there is a strong correlation between some of the parameters. The very high temperature obtained in the canonical *BSQ* ensemble (FCE) correlates with the small radius in the same ensemble. Particle yields increase with temperature but a small volume decreases them, hence the correlation between the parameters.

Table II shows the χ^2 values obtained for the three ensembles considered in this paper. Any one of the methods indicated in the introduction will lead to a lower result for the chi-squared values. Fixing $\gamma_s = 1$ does not change the physics message but considerably worsens the resulting χ^2 values.

The fits to the hadronic yields obtained in *p-p* collisions at 7 TeV in five different centrality bins are shown in Figs. 4 and 5. The upper panels show the yields while the lower panels show the ratios of the measured data divided by the fit values for the three different ensembles considered here. The three lines corresponding to the fits are often very close to each other and overlap, hence they are not always visible on the figures.

IV. DISCUSSION AND CONCLUSIONS

In this paper we have investigated three different ensembles to analyze the variation of particle yields with the multiplicity of charged particles produced in proton-proton collisions at the center-of-mass energy of $\sqrt{s} = 7$ TeV [27], *p*-Pb collisions at 5.02 TeV [28,29], and Pb-Pb collisions at 2.76 TeV [30–32].

We have kept the basic structure of the thermal model as presented in Ref. [24] and focused on the resulting thermal

parameters $T_{\rm ch}$, γ_s and the radius and their dependence on the final-state multiplicity. We note in this regard that recent improvements in the treatment of the particle yields do not lead to substantial changes of the chemical freeze-out temperature $T_{\rm ch}$ [20,22]. Our results show two new interesting features:

1. A comparison of the grand canonical ensemble, the ensemble with strict strangeness conservation and the one with strict baryon number, strangeness, and charge conservation agree very well for large systems such as p-Pb, and Pb-Pb, but show marked differences for p-p collisions. These differences tend to disappear as the multiplicity of charged particles increases in the final state of p-p collisions. This supports the fact that p-p collisions with high multiplicities agree with what is seen in large systems such as Pb-Pb. Quantitatively, this starts happening when there are more than 20 charged hadrons in the midrapidity interval being considered. It also throws doubt on the applicability of the thermal model to low-multiplicity p-p collisions.
2. The convergence of the results in the three ensembles lends support to the notion that a thermodynamic limit is reached where results are independent of the ensemble being used.

We believe that it is of interest to note that all three ensembles lead to the same results when the multiplicity of charged particles $dN_{\rm ch}/d\eta$ exceeds 20 at midrapidity. This could be interpreted as reaching the thermodynamic limit since the three ensembles lead to the same results. It would be of interest to extend this analysis to higher beam energies and higher multiplicity intervals.

ACKNOWLEDGMENTS

One of us (J.C.) gratefully thanks the National Research Foundation of South Africa for financial support. N.S. acknowledges the support of SERB Ramanujan Fellowship (D.O. No. SB/S2/RJN- 084/2015) of the Department of Science and Technology of India. B.H. acknowledges the support of the Université de Strasbourg Institute for Advanced Study.

[1] A. Andronic, P. Braun-Munzinger, K. Redlich, and J. Stachel, Nature **561**, 321 (2018).
[2] R. Stock, F. Becattini, M. Bleicher, and J. Steinheimer, Nucl. Phys. A **982**, 827 (2019).
[3] C. Patrignani *et al.* (Particle Data Group), Chin. Phys. C **40**, 100001 (2016).
[4] J. Cleymans, in *Proceedings, 3rd International Conference on Physics and Astrophysics of Quark-Gluon Plasma (ICPA-QGP '97)*, edited by B. C. Sinha, D. K. Srivastava, and Y. P. Viyogi (Narosa Publishing House, New Delhi, 1998), pp. 55–64.
[5] W. Broniowski and W. Florkowski, Phys. Rev. Lett. **87**, 272302 (2001).
[6] S. V. Akkelin, P. Braun-Munzinger, and Yu. M. Sinyukov, Nucl. Phys. A **710**, 439 (2002).
[7] J. D. Bjorken, Phys. Rev. D **27**, 140 (1983).
[8] J. Noronha-Hostler and C. Greiner, Nucl. Phys. A **931**, 1108 (2014).
[9] M. Petrán, J. Letessier, V. Petráček, and J. Rafelski, Phys. Rev. C **88**, 034907 (2013).
[10] V. Begun, W. Florkowski, and M. Rybczynski, Phys. Rev. C **90**, 014906 (2014).
[11] V. Begun, W. Florkowski, and M. Rybczynski, Phys. Rev. C **90**, 054912 (2014).
[12] J. Steinheimer, J. Aichelin, and M. Bleicher, Phys. Rev. Lett. **110**, 042501 (2013).
[13] F. Becattini, M. Bleicher, T. Kollegger, T. Schuster, J. Steinheimer, and R. Stock, Phys. Rev. Lett. **111**, 082302 (2013).
[14] F. Becattini, J. Steinheimer, R. Stock, and M. Bleicher, Phys. Lett. B **764**, 241 (2017).
[15] S. Chatterjee, R. M. Godbole, and S. Gupta, Phys. Lett. B **727**, 554 (2013).
[16] R. Bellwied, S. Borsanyi, Z. Fodor, S. D. Katz, and C. Ratti, Phys. Rev. Lett. **111**, 202302 (2013).
[17] S. Chatterjee, A. K. Dash, and B. Mohanty, J. Phys. G **44**, 105106 (2017).
[18] R. Bellwied, J. Phys.: Conf. Ser. **736**, 012018 (2016).
[19] P. Alba, V. Vovchenko, M. I. Gorenstein, and H. Stoecker, Nucl. Phys. A **974**, 22 (2018).
[20] V. Vovchenko, M. I. Gorenstein, and H. Stoecker, Phys. Rev. C **98**, 034906 (2018).
[21] A. Dash, S. Samanta, and B. Mohanty, arXiv:1806.02117.
[22] A. Andronic, P. Braun-Munzinger, B. Friman, P. M. Lo, K. Redlich, and J. Stachel, Phys. Lett. B **792**, 304 (2019).
[23] A. Dash, S. Samanta, and B. Mohanty, Phys. Rev. C **97**, 055208 (2018).
[24] S. Wheaton, J. Cleymans, and M. Hauer, Comput. Phys. Commun. **180**, 84 (2009).
[25] P. Braun-Munzinger, J. Cleymans, H. Oeschler, and K. Redlich, Nucl. Phys. A **697**, 902 (2002).
[26] J. Letessier, A. Tounsi, U. W. Heinz, J. Sollfrank, and J. Rafelski, Phys. Rev. D **51**, 3408 (1995).
[27] J. Adam *et al.* (ALICE Collaboration), Nat. Phys. **13**, 535 (2017).
[28] B. B. Abelev *et al.* (ALICE Collaboration), Phys. Lett. B **728**, 25 (2014).
[29] J. Adam *et al.* (ALICE Collaboration), Phys. Lett. B **758**, 389 (2016).
[30] B. Abelev *et al.* (ALICE Collaboration), Phys. Rev. C **88**, 044910 (2013).
[31] B. B. Abelev *et al.* (ALICE Collaboration), Phys. Rev. Lett. **111**, 222301 (2013).
[32] B. B. Abelev *et al.* (ALICE Collaboration), Phys. Lett. B **728**, 216 (2014); B. B. Abelev *et al.*, **734**, 314 (2014).
[33] B. I. Abelev *et al.* (STAR Collaboration), Phys. Rev. C **75**, 064901 (2007).
[34] F. Becattini, P. Castorina, A. Milov, and H. Satz, J. Phys. G **38**, 025002 (2011).
[35] F. Becattini, P. Castorina, A. Milov, and H. Satz, Eur. Phys. J. C **66**, 377 (2010).
[36] V. Vislavicius and A. Kalweit, arXiv:1610.03001.
[37] N. Sharma, J. Cleymans, and L. Kumar, Eur. Phys. J. C **78**, 288 (2018).
[38] A. Bazavov *et al.*, arXiv:1812.08235.